Pyrene-Cored Covalent Organic Polymers by Thiophene-Based Isomers, Their Gas Adsorption, and Photophysical Properties

Changfeng Li,[1] Peixian Li,[1,2] Linjiang Chen,[3] Michael E. Briggs ,[3] Ming Liu ,[3] Kai Chen,[2] Xiaoxiao Shi,[2] Deman Han,[2] Shibin Ren[2,3]

[1]School of Chemistry and materials Science, Shanxi Normal University, Lin Fen 041004, China
[2]School of Pharmaceutical and Chemical Engineering, Taizhou University, Taizhou 317000, China
[3]Materials Innovation Factory and Department of Chemistry, University of Liverpool, Liverpool L69 7ZD, UK
Correspondence to: S. Ren (E-mail: renshibin@126.com)

Received 19 February 2017; accepted 8 April 2017; published online 7 May 2017
DOI: 10.1002/pola.28627

ABSTRACT: Two new pyrene-cored covalent organic polymers (COPs), **CK-COP-1** and **CK-COP-2**, were synthesized via the one-step polymerization of two thiophene-based isomers, 1,3,6,8-tetra(thiophene-2-yl) pyrene (**L_1**) and 1,3,6,8-tetra(thiophene-3-yl) pyrene (**L_2**). The resulting pyrene-cored COPs exhibit rather different surface areas of 54 m^2 g^{-1} and 615 m^2g^{-1} for **CK-COP-1** and **CK-COP-2**, respectively. The CO_2 uptake capacities of **CK-COP-1** and **CK-COP-2** also show different values of 2.85 and 9.73 wt % at 273 K, respectively. Furthermore, **CK-COP-2** offers not only a larger CO_2 adsorption capacity but also a better CO_2/CH_4 selectivity at 273 K compared with **CK-COP-1**. **CK-COP-1** and **CK-COP-2** also exhibit considerable differences in their photophysical property. The different structure and properties of **CK-COPs** could be attributed to the isomer effect of their corresponding thiophene-based monomers. © 2017 Authors. Journal of Polymer Science Part A: Polymer Chemistry Published by Wiley Periodicals, Inc. J. Polym. Sci., Part A: Polym. Chem. **2017**, *55*, 2383–2389

KEYWORDS: covalent organic polymers (COPs); gas adsorption; photophysical properties; thiophene-based isomers

INTRODUCTION Anthropogenic carbon dioxide (CO_2) emissions have been linked to rising global temperatures and extreme weather events. Reducing the level of these emissions by switching to green energy production combined with efficient CO_2 capture and sequestration can lessen the negative effect on our environment.[1] To date, only a few technologies like amine scrubbing have been commercialized for CO_2 capture and separation. However, regeneration of the amine scrubber requires significant energy expenditure while exposure to the amine solution can result in severe corrosion of equipment and pipework.[2,3] Over the past decade, metal-organic frameworks (MOFs) have generated considerable interest as carbon capture materials due to their high specific surface area and excellent adsorption capability.[4–8] Nevertheless, the presence of weak coordination bonds in these MOFs can lead to some severe drawbacks such as low stability and water affinity. Covalent organic polymers (COPs), constructed from strong covalent bonds have demonstrated superior thermal and chemical stability. In particular, these porous materials can reversibly adsorb and release CO_2 via physisorption as opposed to the chemisorption mechanism of the amine scrubbers, which results in a lower energy penalty for regeneration. The combination of high permanent porosity, readily functionalized pores, and well-tuned pore size distributions means that COPs have the potential to be CO_2 adsorbent materials of the future.[9–11] The incorporation of CO_2-philic functional groups into the polymers by bottom-up or post-synthesis approach allows COPs to be tailored toward specific applications.[12] The incorporation of non-classical reactive sites such as carboxyl, triazine, benzimidazole, carbazole, hydroxyl, imine, and so forth, into COPs has proved beneficial for CO_2 uptake.[13–19] Ionic functionality present in the polymers can also improve CO_2 capture due to the polarization of guest molecules.[20,21] Depending on the functionality present these porous organic polymers can be classified as porous aromatic frameworks,[22,23] covalent triazine polymers,[14] carbazole-based microporous polymers,[15] benzimidazole-linked polymers,[16,17] and porous imine-linked networks.[19] With the exception of the COPs decorated with these polar groups, only a few non-polarizable COPs, such as porous aromatic framework (PAF-1)[22] and a number of the porous polymer networks (PPN)

Additional Supporting Information may be found in the online version of this article.

polymers[23] exhibit excellent CO_2 adsorption and separation. However, the preparation of extended conjugated COPs by two isomeric thiophene substituted pyrenes has not been reported to date.

In recent years, pyrene-based porous materials have been widely used in various fields, such as photo-catalysis, photoelectric devices, chemical sensing, gas storage and separation, and degradation of nerve agent simulants due to their excellent rigidity and photophysical properties.[24–28] It has also been observed that changes in spatial configuration or conformation of isomeric ligands can have a great influence on the structures and properties of the final coordination polymers.[29,30] Motivated by all the above, we selected two isomeric monomers in which a thiophene ring is attached at either the 2- or 3- position to pyrene at its 1-, 3-, 6-, and 8-positions. Oxidative polymerization of the two thiophene containing monomers afforded porous fluorescent COPs. The position of attachment of the thiophene to the pyrene core changes the number of reactive sites for polymerisation and will result in differences in the spatial configuration or orientation of the thiophene in the final polymers. Thiophene derivatized pyrenes can exhibit longer adsorption and emission wavelengths as well as high fluorescent quantum yields, compared with pyrene itself.[31] The incorporation of these monomers into a network will greatly affect charge distribution within the extended conjugated frameworks. In this article, we reported the synthesis of two pyrene-cored COPs, **CK-COP-1** and **CK-COP-2**, derived from 1,3,6,8-tetra- (thiophene-2-yl)pyrene (**L_1**) and 1,3,6,8-tetra(thiophene-3-yl)pyrene (**L_2**), respectively. In addition, the gas adsorption and photophysical properties of the two isomeric polymers are also studied.

EXPERIMENTAL

Materials and Methods

1,3,6,8-Tetrabromopyrene was synthesized according to the literature method.[32] Pyrene, 2-thienylboronic acid, and 3-thienylboronic acid were purchased from Sigma Aldrich. All other chemicals were from commercial sources and used without further purification.

^{1}H NMR spectra of **L_1** and **L_2** were tested on Bruker advance 400 MHz NMR spectrometer. Solid-state ^{13}C CP/MAS NMR spectra of the polymers were measured on a Bruker Advance II WB 400 MHz NMR spectrometer using a 4-mm DVT CP/MAS probe at a MAS rate of 10 kHz. Fourier-transform infrared (FTIR) spectroscopy was performed on Bruker Vector spectrophotometer using KBr pellets and measured over the range of 4000–400 cm^{-1}. Thermogravimetric analysis (TGA) was collected on TGA/SDT-Q600 under a nitrogen atmosphere at a heating rate of 10 °C min^{-1}. Powder X-ray diffraction (PXRD) was carried out on Bruker D8 advance X-diffractometer with Cu-Kα radiation. Scanning electron microscopy (SEM) was performed on an S-4800 (Hitachi Ltd) field emission SEM. Gas adsorption–desorption isotherms were collected by volumetric method on a Micromeritics ASAP 2020 HD88 instrument. The samples were degassed at 423 K under dynamic vacuum for 12 h. The specific surface area and pore size distribution were calculated from the N_2 adsorption at 77 K using the Brunauer-Emmett-Teller (BET) method and non-local density functional theory (NLDFT) method, respectively. CO_2 and CH_4 adsorption–desorption isotherms were tested at 273 and 298 K up to 1 bar. Photoluminescence analysis was performed on a Hitachi 850 fluorescence spectrophotometer. The solid state UV-Visible absorption was recorded on a Shimadzu UV-2550 UV-Vis spectrometer.

Synthesis of CK-COPs

Synthesis of 1,3,6,8-tetra(thiophene-2-yl)pyrene (**L_1**)

In a 250-mL three-necked round-bottomed flask, the reaction mixture of tetrabromopyrene (3.12 g, 6 mmol), 2-thienylboronic acid (4.61 g, 36 mmol), palladium tetrakis(triphenylphosphine) (0.36 g, 0.30 mmol), and potassium carbonate (6.30 g, 45 mmol) were stirred in anhydrous dioxane (60 mL) under a nitrogen atmosphere for 3 days at 85 °C. After cooling to ambient temperature, the yellow reaction mixture was transferred to a solution of cold concentrated HCl solution (100 mL). The precipitate was collected by filtration and then washed with 2 M HCl (3 × 40 mL). The solid was transferred to a Soxhlet and continuously extracted with $CHCl_3$ for 24 h. The $CHCl_3$ extracts were dried over $MgSO_4$, filtered, and evaporated under reduced pressure. The crude product **L_1** was further recrystallized from hot $CHCl_3$ to afford **L_1** as a bright yellow powder (2.11 g, 66%). ^{1}H NMR (400 MHz d_6-DMSO): δ (ppm) 8.57 (s, 4H), 8.21 (s, 2H), 7.87 (dd, J = 5.2, 1.2 Hz, 4H), 7.58 (dd, J = 3.4, 1.0 Hz, 4H), 7.37 (dd, J = 5.2, 3.6 Hz, 4H). ^{13}C NMR (400 MHz $CDCl_3$): δ (ppm) 141.86, 131.23, 129.77, 129.12, 128.37, 127.54, 126.52, 125.88, 125.76. FT-IR (ATR 4000–400 cm^{-1}) 3418, 3086, 2927, 1800, 1603, 1495, 1462, 1430, 1385, 1272, 1236, 1207, 1076, 1044, 948, 905, 850, 830, 814, 702, 686, 597. MS (ESI): m/z for $C_{32}H_{18}S_4$ cacld 530.03, M^+ 530.1.

Synthesis of 1,3,6,8-tetra(thiophene-3-yl)pyrene (**L_2**)

Apart from 3-thienylboronic acid, the preparation method of **L_2** was the same to that of **L_1**. Its yield was 1.95 g (61%). ^{1}H NMR (400 MHz $CDCl_3$): δ (ppm) 8.31 (s, 4H), 8.09 (s, 2H), 7.55 (dd, J = 2.8, 1.2 Hz, 4H), 7.53 (dd, J = 4.8, 2.8 Hz, 4H), 7.47 (dd, J = 4.8, 1.2 Hz, 4H). ^{13}C NMR (400 MHz $CDCl_3$): δ (ppm) 141.39, 132.02, 130.00, 129.36, 128.47, 125.94, 125.59, 125.31, 124.12. FT-IR (ATR 4000–400 cm^{-1}) 3468, 3091, 2903, 1803, 1607, 1485, 1462, 1385, 1338, 1272, 1204, 1076, 912, 902, 886, 860, 837, 797, 781, 732, 702, 676, 647, 542. MS (ESI): m/z for $C_{32}H_{18}S_4$ cacld 530.03, M^+ 530.2.

Synthesis of CK-COP-1

In a classical synthesized procedure, anhydrous $FeCl_3$ (0.81 g, 5.00 mmol) was added to a 250-mL three-necked round-bottomed flask containing 20 mL dried $CHCl_3$ under N_2 atmosphere. **L_1** (0.13 g, 0.25 mmol) was dissolved in anhydrous $CHCl_3$ (20 mL) and added dropwise over 1 h to the $FeCl_3$ suspension at room temperature with continuous stirring. During the addition of **L_1**, the reaction mixture quickly changed from dark green to black with the appearance of a precipitate. The mixture was stirred under a N_2

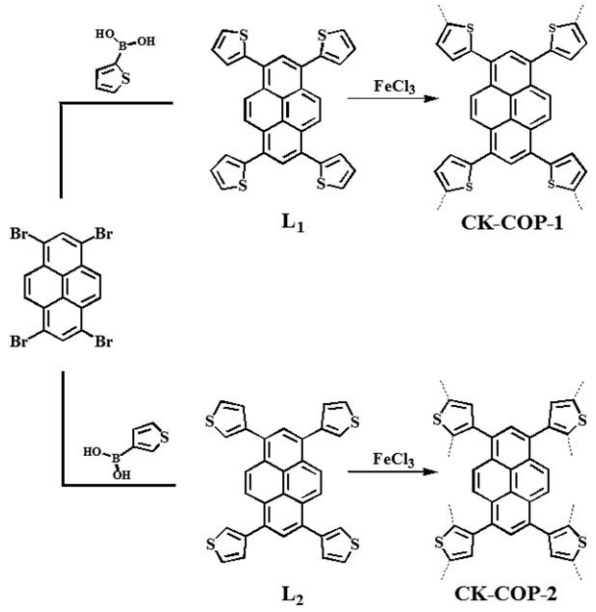

SCHEME 1 The synthesis of CK-COP-1 and CK-COP-2.

atmosphere for a further 24 h. The suspension was poured into methanol (100 mL), stirred for 1 h, filtered, and washed with methanol (3 × 20 mL) to yield an orange-red solid. The solid was added to a cold solution of concentrated hydrochloric acid (50 mL) and stirred for 2 h. It was filtered, washed with water (3 × 20 mL), methanol (3 × 20 mL), and then washed via Soxhlet extraction with THF and methanol successively for 24 h. Finally, the purified **CK-COP-1** was vacuum-dried in an oven at 100 °C for 12 h to afford a bright orange-red solid (0.055 g, 42%).

Synthesis of **CK-COP-2**: The same procedure mentioned above was followed using the precursor $\mathbf{L_2}$ instead of $\mathbf{L_1}$. The final product was isolated as a dark red solid with a yield of 0.049 g (38%).

RESULTS AND DISCUSSION

The two **COPs**, **CK-COP-1** and **CK-COP-2**, were prepared by oxidative polymerization of the thiophene containing monomers, $\mathbf{L_1}$ or $\mathbf{L_2}$, with $FeCl_3$. $\mathbf{L_1}$ and $\mathbf{L_2}$ were synthesized via the fourfold Suzuki cross-coupling of 2-thienylboronic acid or 3-thienylboronic acid with tetrabromopyrene (Scheme 1).[33] **CK-COP-1** and **CK-COP-2** were characterized by FTIR spectroscopy, TGA, PXRD, SEM, and solid-state ^{13}C NMR. Additionally, their porosity was investigated by the gas adsorption–desorption measurements.

The FTIR spectrum of the two monomers and their corresponding polymers is depicted in Figure 1. In the two monomers, three peaks at 1462, 1385, and 1207 cm^{-1} were attributed to the stretching vibration of C=C and C—C bonds from the thiophene units.[34] The vibration peaks of C—S—C bonds from the thiophene units appear at 702 cm^{-1} for the monomer $\mathbf{L_1}$ and 729 cm^{-1} for the monomer $\mathbf{L_2}$, respectively. The peaks corresponding to the C=C and C—C bonds in the two polymers were comparable with that of the monomers. However, the peak intensities at 702 and 729 cm^{-1} in monomers $\mathbf{L_1}$ and $\mathbf{L_2}$, respectively, which can be attributed to the aromatic C—H out-of-plane bending vibrations within thiophene structures decrease on polymerisation.[35] CK-COP-2 exhibits more obvious drop in the FT-IR intensity than CK-COP-1, which indicates that the CK-COP-2 are more completely polymerized that CK-COP-1. Solid-state ^{13}C CP/MAS NMR spectrum was also used to confirm their structure of the two COPs (Fig. 2). For **CK-COP-1**, the peak at about 141 ppm was assigned as the carbon atoms attached to the S atom in the thiophene rings and the overlapping peaks at about 127 ppm were assigned to the pyrene carbons and the remaining thiophene carbons.[36] Meanwhile, for **CK-COP-2**, the shoulder peak at 146 ppm was assigned to the thiophene carbon directly linked to the pyrene cores, while the broad peak from 115 to 145 ppm was assigned to the pyrene carbons and the remaining thiophene carbons. The differences between **CK-COP-1** and **CK-COP-2**, observed by IR and solid state NMR, originate from the different connection modes between pyrene cores and thiophene units in the polymers.

The insoluble nature of both CK-COPs in common organic solvents is also indicative of the formation of well-established 3D frameworks. TGA of the two polymers revealed obvious differences in the thermal stability. Whereas **CK-COP-1** displayed little mass loss up at about 500 °C, **CK-COP-2** displays a pronounced mass loss from about 200 °C (Supporting Information Fig. S1). For **CK-COP-1**, the SEM micrographs (Supporting Information Fig. S2) showed the formation of particulate structure whereas the SEM micrographs of CK-COP-2 (Supporting Information Fig. S3) showed a nanofiber morphology. There were no obvious crystallinity as suggested by their PXRD patterns (Supporting Information Fig. S4), indicating the amorphous nature of the two materials.

To investigate the porosities of the CK-COPs, N_2 adsorption–desorption measurements at 77 K up to 1 bar pressure were performed. Before analysis, the polymers were degassed under

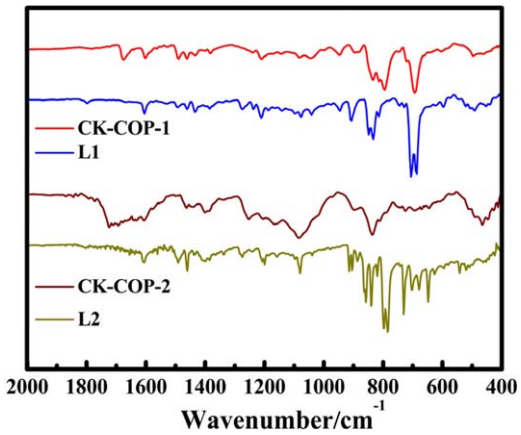

FIGURE 1 FTIR spectra of **CK-COP-1** and **CK-COP-2** and their corresponding monomer $\mathbf{L_1}$ and $\mathbf{L_2}$. [Color figure can be viewed at wileyonlinelibrary.com]

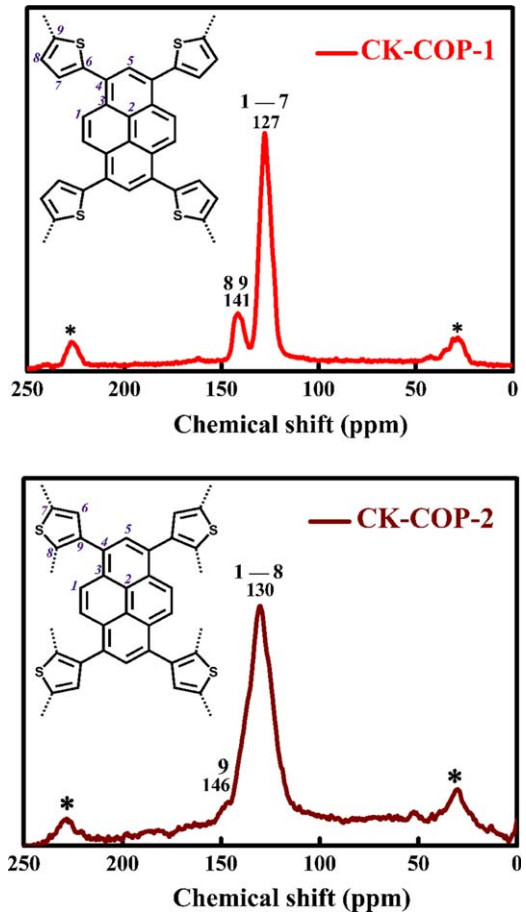

FIGURE 2 Solid-state ^{13}C CP/MAS NMR spectrum of **CK-COP-1** and **CK-COP-2**. [Color figure can be viewed at wileyonlinelibrary.com]

dynamic vacuum at 423 K for 12 h. As shown in Figure 3(A), **CK-COP-1** displays very low N_2 adsorption across the whole pressure range. This phenomenon can be related with the tight packing structure of the prepared polymer (Supporting Information Fig. S2), which blocks nitrogen gas from entering the pore channel at low temperature. However, the fully reversible isotherms of **CK-COP-2** show a rapid nitrogen uptake at low pressure ($P/P_0 < 0.05$), indicative of a permanent microporous structure.[37] The gradual increase in N_2 uptake and the minor hysteresis suggest the presence of mesopores, which may originate from the loose nanofibers structure and swelling of the polymer (Supporting Information Fig. S3).[38] Applying the Brunauer–Emmett–Teller model within the pressure range of $P/P_0 = 0.01$–0.2 results in an apparent surface area (SA_{BET}) of 54 $m^2\ g^{-1}$ for **CK-COP-1** and 615 $m^2\ g^{-1}$ for **CK-COP-2**. Moreover, total volumes were calculated from the single point N_2 uptake ($P/P_0 = 0.99$) and found to be 0.33 $cm^3\ g^{-1}$ (**CK-COP-1**) and 0.68 $cm^3\ g^{-1}$ (**CK-COP-2**). The pore size distribution of the two materials were evaluated by fitting the adsorption branches of the N_2 isotherms using the NLDFT and found to be centered around 1.02 nm (**CK-COP-1**) and 0.52 nm (**CK-COP-2**) [Fig. 3(B)]. As depicted in Supporting Information Table S1, the differences in the SA_{BET}, total volume, and pore size distribution between the two CK-COPs are closely associated with the different substitution patterns in the monomers. For **CK-COP-1**, $\mathbf{L_1}$ possesses only one reactive site adjacent to the sulfur atom in the thiophene ring, which will result in a lower degree of crosslinking and result in a tightly packed structure (Supporting Information Fig. S2). Whereas for **CK-COP-2**, $\mathbf{L_2}$ possesses two reactive sites adjacent to the sulfur atom in the thiophene ring, resulting in a higher degree of crosslinking and therefore a more open structure than that observed for **CK-COP-1**.

In view of the fact that the CK-COPs possess different structural characteristics, the CO_2 uptake and the CO_2/CH_4 selectivity were performed. Both separations are industrially relevant for the upgrade and purification of nature gas and flue gas, respectively. The adsorption–desorption isotherms of CO_2 and CH_4 were recorded up to 1 bar at 273 and 298 K (Fig. 4; Supporting Information Fig. S5). The CO_2 and CH_4 sorption isotherms of CK-COPs are shown in Figure 4(A,C) and Supporting Information Figure S5 at low pressure and show reversible adsorption up to 1 bar, which implies that the guest loaded CK-COPs can be cost-effectively regenerated via a pressure swing mechanism. It was observed that both CK-COPs do not reach the saturation at 1 bar. **CK-COP-1** and **CK-COP-2**

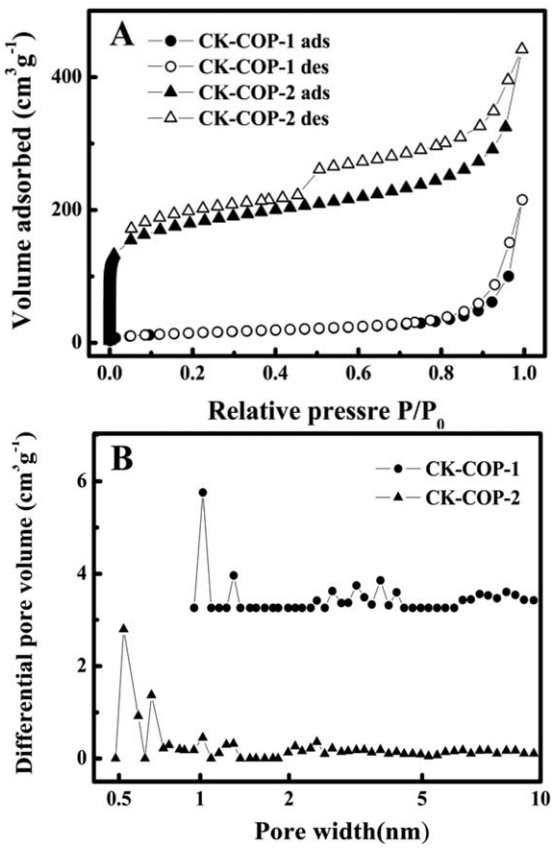

FIGURE 3 (A) N_2 adsorption/desorption isotherms at 77 K for **CK-COP-1** and **CK-COP-2**. The filled and open symbols represent adsorption and desorption, respectively; (B) Pore size distribution of **CK-COPs**.

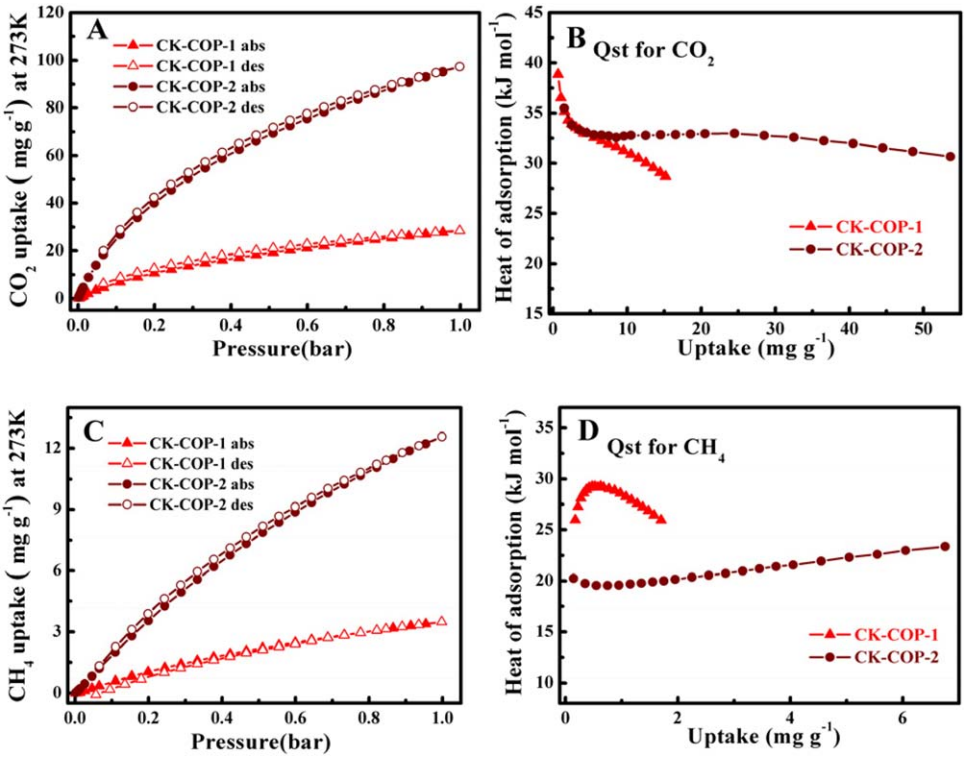

FIGURE 4 (A) CO_2 and (C) CH_4 adsorption/desorption isotherms at 273 K for **CK-COP-1** and **CK-COP-2**. The filled and open symbols represent adsorption and desorption, respectively. Isosteric heat for (B) CO_2 and (D) CH_4 adsorption for **CK-COP-1** and **CK-COP-2**. [Color figure can be viewed at wileyonlinelibrary.com]

show CO_2 uptakes of 2.85 and 9.73 wt %, respectively, at 273 K and 1 bar. In addition, although their values are lower than those of reported porous materials, such as hydroxyl functionalized porous organic frameworks (POFs) (18.40 wt %),[18] imine-linked porous polymers PPF-1 (18.40 wt %)[39] and pyrene-derived benzimidazole-linked polymers BILP-10 (17.70 wt %),[16] the CO_2 adsorption value for **CK-COP-2** (9.73 wt %) compares favorably with that of other reported porous adsorbents such as porous electron-rich covalent organonitridic frameworks (PECONF-1) (8.2 wt %),[9] conjugated microporous polymer (CMP-1) (9.02 wt %),[13] imine-linked polymer (ILP) (8.67 wt %),[40] triazine-framework-based porous membranes (TFM-1) (7.6 wt %),[41] and porous aromatic framework (PAF-1) (9.2 wt %).[42] The CH_4 sorption of CK-COPs was also assessed up to 1 bar at 273 and 298 K (Fig. 4C). The CH_4 capacities are 0.35 and 1.25 wt % for **CK-COP-1** and **CK-COP-2**, respectively, at 273 K. The difference in CO_2 and CH_4 uptake capacity is consistent with the measured surface area and pore volume for the two polymers and can be attributed to differences in their structures caused by different degrees of their crosslinking.

A moderate enthalpy of CO_2 adsorption (Q_{st}) is beneficial for the development of porous adsorbents.[9] The isosteric heat of CO_2 and CH_4 adsorption (Q_{st}) was calculated from their corresponding adsorption isotherms at 273 and 298 K, respectively, using the Clausius–Clapeyron equation. As exhibited in Figure 3B, at the zero coverage, the isosteric heats of CO_2 adsorption were 38.8 kJ mol^{-1} for **CK-COP-1** and 35.5 kJ mol^{-1} for **CK-COP-2**. It was observed that the Q_{st} for **CK-COP-1** rapidly decreased with CO_2 loading. In sharp contrast, the Q_{st} for **CK-COP-2** remains consistent up to a loading of 50 mg g^{-1}. The Q_{st} for CO_2 uptake in **CK-COP-1** and **CK-COP-1** is within the range observed for other organic porous polymers such as PECONFs (26.0–34.0 kJ mol^{-1}),[9] BILPs (31.2–35.8 kJ mol^{-1}),[17] and PPFs (21.8–29.2 kJ mol^{-1}),[39] and are slightly below the value suggestive of chemisorption (40 kJ mol^{-1}), indicating physical adsorption of the CO_2 on to the pore wall. The co-existence of both thiophene and pyrene within the polymers leads to a highly conjugated electron rich structure, which can benefit the CO_2 adsorption via Lewis acid–Lewis base interactions. The maximum isosteric heat of CH_4 adsorption in **CK-COP-1** and **CK-COP-2** reach 29.2 and 20.0 kJ mol^{-1}, respectively [Fig. 3(D)]. To evaluate the CO_2/CH_4 separation performances of CK-COPs, the selectivity of CO_2 over CH_4 was also calculated using the ideal adsorbed solution theory (IAST), based on the experimental pure-gas isotherms at 298 K and 1 bar. The adsorption selectivity for CO_2/CH_4 mixtures (15/85 molar ratio) of **CK-COP-1** and **CK-COP-2** as a function of pressure is shown in Supporting Information Figure S6. CK-COP-2 has better CO_2/CH_4 selectivity than CK-COP-1 at 273 K, but not such at 298 K.

In addition, the photophysical properties of **L_1**, **L_2**, and **CK-COPs** have also been investigated in CH_2Cl_2 at room temperature and the results are shown in Figure 5. The emission

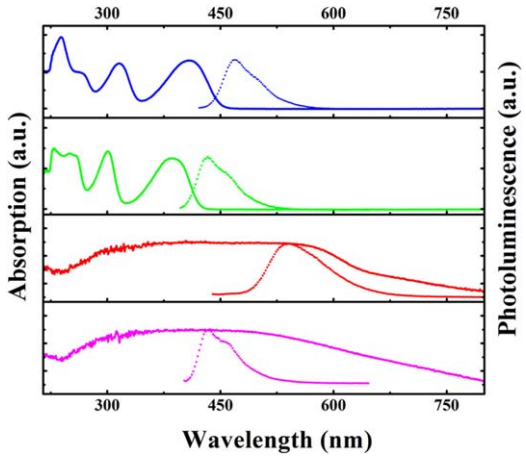

FIGURE 5 UV-Vis spectra (solid line) and emission spectra (dot line) of the monomers and the corresponding polymers ($\mathbf{L_1}$, $\mathbf{L_2}$, **CK-COP-1**, and **CK-COP-2**) upon excitation at 407 nm, 390 nm, 433 nm, and 395 nm (from top to bottom). [Color figure can be viewed at wileyonlinelibrary.com]

spectra for $\mathbf{L_1}$, $\mathbf{L_2}$, **CK-COP-1**, and **CK-COP-2** exhibited maximum emission bands at 470, 432, 540, and 433 nm, respectively. The emission wavelength of **CK-COP-1** is red-shifted by ~70 nm, compared with that of $\mathbf{L_1}$. The red shift could be due to the enhanced planar conformation and extended π-conjugation framework for **CK-COP-1**. By contrast, the emission peaks of **CK-COP-2** and $\mathbf{L_2}$ almost overlap at 433 nm. Such a phenomenon for **CK-COP-2** and $\mathbf{L_2}$ is perhaps ascribed to a high degree of crosslinking and low extent of π-orbital overlap since the two reactive sites of $\mathbf{L_2}$ are not equivalent.

Additionally, the emission spectra and UV-Vis spectra of $\mathbf{L_1}$ and $\mathbf{L_2}$ are rather similar but different in wavelength, perhaps in that $\mathbf{L_1}$ can be endowed with the more planar structure and more extended π-conjugated system than $\mathbf{L_2}$ even though both monomers are isomers. The position of the thiophene attached on pyrene units changes the number of reactive sites for oxidative polymerization, which will control the orientation and distribution of thiophenes within the resulting polymers. Therefore, it is believed that all these differences in the photophysical properties of COPs could be attributable to their different structures due to the orientation and distribution of thiophenes on pyrene cores within the resulting polymers.

CONCLUSIONS

The two COPs were successfully prepared via the oxidative polymerisation of two isomeric thiophene substituted pyrenes. Differences in the attachment of the thiophene rings to the pyrene core result in greater crosslinking in **CK-COP-2** than for **CK-COP-1**. The high degree of crosslinking in **CK-COP-2** results in a more rigid structure that results in the thiophene twisting out of plane with the pyrene. The difference in structure between the two polymers is consistent with the observed porosity, gas uptakes, and photophysical properties of the two polymers.

ACKNOWLEDGMENTS

This work was supported by the National Natural Science Foundation of China (21471110, 21575097, and 21375092).

REFERENCES AND NOTES

1 Q. Wang, J. Luo, Z. Zhong, A. Borgna, *Energy Environ. Sci.* **2011**, *4*, 42–55.

2 G. T. Rochelle, *Science.* **2009**, *325*, 1652–1654.

3 A. Goeppert, M. Czaun, G. K. Surya Prakash, G. A. Olah, *Energy Environ. Sci.* **2012**, *5*, 783–7853.

4 A. C. Sudik, A. R. Millward, N. W. Ockwig, A. P. Côté, J. Kim, O. M. Yaghi, *J. Am. Chem. Soc.* **2005**, *127*, 7110–7118.

5 X.-S. Wang, S. Ma, D. Sun, S. Parkin, H.-C. Zhou, *J. Am. Chem. Soc.* **2006**, *128*, 16474–16475.

6 M. Xue, S. Ma, Z. Jin, R. M. Schaffino, G.-S. Zhu, E. B. Lobkovsky, S.-L. Qiu, B. Chen, *Inorg. Chem.* **2008**, *47*, 6825–6828.

7 A. Sonnauer, F. Hoffmann, M. Frba, L. Kienle, V. Duppel, M. Thommes, C. Serre, G. Férey, N. Stock, *Angew. Chem. Int. Ed.* **2009**, *48*, 3791–3794.

8 R.-B. Lin, F. Li, S.-Y. Liu, X.-L. Qi, J.-P. Zhang, X.-M. Chen, *Angew. Chem. Int. Ed.* **2013**, *52*, 13429–13433.

9 P. mohanty, L. D. Kull, K. Landskron, *Nat. Commun.* **2011**, *2*, 401–406.

10 J.-X. Jiang, F. Su, A. Trewin, C. D. Wood, N. L. Campbell, H. Niu, C. Dickinson, A. Y. Ganin, M. J. Rosseinsky, Y. Z. Khimyak, A. I. Cooper, *Angew. Chem. Int. Ed.* **2007**, *46*, 8574–8578.

11 Y. Xu, S. Jin, H. Xu, A. Nagai, D. Jiang, *Chem. Soc. Rev.* **2013**, *42*, 8012–8031.

12 Z. Xiang, D. Cao, *J. Mater. Chem. A.* **2013**, *1*, 2691–2718.

13 R. Dawson, D. J. Adams, A. I. Cooper, *Chem. Sci.* **2011**, *2*, 1173–1177.

14 A. Bhunia, V. Vasylyeva, C. Janiak, *Chem. Commun.* **2013**, *49*, 3961–3963.

15 Q. Chen, M. Luo, P. Hammershøj, D. Zhou, Y. Han, B. W. Laursen, C.-G. Yan, B.-H. Han, *J. Am. Chem. Soc.* **2012**, *134*, 6084–6087.

16 M. G. Rabbani, A. K. Sekizkardes, O. M. El-Kadri, B. R. Kaafarani, H. M. El-Kaderi, *J. Mater. Chem.* **2012**, *22*, 25409–25417.

17 A. K. Sekizkardes, T. İslamŏglu, Z. Kahveci, H. M. El-Kaderi, *J. Mater. Chem. A.* **2014**, *2*, 12492–12500.

18 A. P. Katsoulidis, M. G. Kanatzidis, *Chem. Mater.* **2011**, *23*, 1818–1824.

19 N. Popp, T. Homburg, N. Stock, J. Senker, *J. Mater. Chem. A.* **2015**, *3*, 18492–18504.

20 J. S. Lee, H. Luo, G. A. Baker, S. Dai, *Chem. Mater.* **2009**, *21*, 4756–4758.

21 S. Soll, Q. Zhao, J. Weber, J. Yuan, *Chem. Mater.* **2013**, *25*, 3003–3010.

22 T. Ben, H. Ren, S. Ma, D. Cao, J. Lan, X. Jing, W. Wang, J. Xu, F. Deng, J. M. Simmons, S. Qiu, G. Zhu, *Angew. Chem., Int. Ed.* **2009**, *48*, 9457–9460.

23 W. Lu, D. Yuan, D. Zhao, C. I. Schilling, O. Plietzsch, T. Muller, S. Bräse, J. Guenther, J. Blümel, R. Krishna, Z. Li, H. C. Zhou, *Chem. Mater.* **2010**, *22*, 5964–5972.

24 G. Lin, H. Ding, D. Yuan, B. Wang, C. Wang, *J. Am. Chem. Soc.* **2016**, *138*, 3302–3305.

25 M. G. Rabbani, A. K. Sekizkardes, Z. Kahveci, T. E. Reich, R. Ding, H. M. El-Kaderi, *Chem. Eur. J.* **2013**, *19*, 3324–3328.

26 S. Wan, J. Guo, J. Kim, H. Ihee, D. Jiang, *Angew. Chem. Int. Ed.* **2009**, *48*, 5439–5442.

27 R. S. Sprick, J.-X. Jiang, B. Bonillo, S. Ren, T. Ratvijitvech, P. Guiglion, M. A. Zwijnenburg, D. J. Adams, A. I. Cooper, *J. Am. Chem. Soc.* **2015**, *137*, 3265–3270.

28 S. Dalapati, S. Jin, J. Gao, Y. Xu, A. Nagai, D. Jiang, *J. Am. Chem. Soc.* **2013**, *135*, 17310–17313.

29 S.-B. Ren, L. Zhou, J. Zhang, Y.-Z. Li, H.-B. Du, X.-Z. You, *CrystEngComm.* **2009**, *11*, 1834–1836.

30 S. B. Ren, Z. J. Qiu, J. Yan, S. L. Zhao, C. L. Wu, W. P. Jia, D. M. Han, H.-D. Liang, *J. Mol. Struct.* **2013**, *23*, 15–20.

31 T. M. Figueira-Duarte, K. Müllen, *Chem. Rev.* **2011**, *111*, 7260–7314.

32 G. Venkataramana, S. Sankararaman, *Eur. J. Org. Chem.* **2005**, 4162–4166.

33 H. Zhang, Y. Wang, K. Shao, Y. Liu, S. Chen, W. Qiu, X. Sun, T. Qi, Y. Ma, G. Yu, Z. Su, D. Zhu, *Chem. Commun.* **2006**, 755–757.

34 C. Kvarnström, H. Neugebauer, S. Blomquist, H. J. Ahonen, J. Kankare, A. Ivaska, *Electrochim. Acta.* **1999**, *44*, 2739–2750.

35 J. Wang, *Electrochimica Acta.* **1994**, *39*, 417–429.

36 S. K. Kundu, A. Bhaumik, *ACS Sustainable Chem. Eng.* **2016**, *4*, 3697–3703.

37 X. Zhang, J. Lu, J. Zhang, *Chem. Mater.* **2014**, *26*, 4023–4029.

38 P. M. Budd, E. S. Elabas, B. S. Chanem, S. Makhseed, N. B. Makeown, K. J. Msayib, C. E. Tattershall, D. Wang, *Adv. Mater.* **2004**, *16*, 456–459.

39 Y. Zhu, H. Long, W. Zhang, *Chem. Mater.* **2013**, *25*, 1630–1635.

40 X. Zhu, C. Tian, S. M. Mahurin, S. H. Chai, C. Wang, S. Brown, G. M. Veith, H. Luo, S. Dai, *J. Am. Chem. Soc.* **2012**, *134*, 10478–10484.

41 T. Ben, C. Pei, D. Zhang, J. Xu, F. Deng, X. Jing, S. Qiu, *Energy Environ. Sci.* **2011**, *4*, 3991–3999.

42 J. Wang, I. Senkovska, M. Oschatz, M. R. Lohe, L. Borchardt, A. Heerwig, Q. Liu, S. Kaskel, *ACS Appl. Mater. Interfaces* **2013**, *5*, 3160–3167.